

Heat and mass transfer studies on water–lithium bromide absorption heat pump systems

M. A. R. EISA

20 Rabaa Adwia, Nasr City, Cairo, Egypt

(Received 15 January 1990 and in final form 4 May 1990)

INTRODUCTION

ABSORPTION heat pump systems basically consist of an evaporator, a condenser, a generator and an absorber.

The working fluid extracts an amount of heat Q_{EV} from the source and evaporates at a temperature T_{EV} .

The pressure of the working fluid is then increased in the absorption circuit before it is condensed in the condenser where it gives up an amount of heat Q_{CO} at a higher temperature T_{CO} . The condensed working fluid is then expanded through the expansion valve and returned to the evaporator to complete the cycle.

The absorption circuit consists of a generator, an absorber and an economizer. Figure 1 shows a schematic diagram for an absorption heat pump system.

The coefficient of performance of an absorption heat pump system is mainly dependent on the efficiencies of the absorption, evaporation, condensation and heat exchanging process which are basically the heat and mass transfer efficiencies.

Comprehensive procedures for the calculation of mass transfer rates have been given by Spalding [1] for different conditions. The rate of heat exchange through the absorption process is a function of the overall coefficient of the heat transfer U , the area of transfer and the temperature difference driving force ΔT

$$Q_{AB} = UAT_{LM}. \quad (1)$$

Gabsi and Bugrel [2] estimated the overall heat transfer coefficient for a wetted wall column with tangential feed for the absorption of water vapour by aqueous lithium bromide solution. They related the overall heat transfer coefficient to the vapour and the liquid flow rates by the following equation:

$$U = 0.0185M_V^{0.94}M_L^{0.133}. \quad (2)$$

With reference to Fig. 1, the role of the absorber is to replace the compressor used in a mechanical vapour, e.g. water vapour from the evaporator is absorbed in an absorbent solution in the absorber generating heat at rate Q_{AB} and temperature T_{AB} . The working fluid rich solution is then pumped from a pressure P_{EV} in the absorber to a pressure P_{CO} in the generator at temperature T_{GE} . A heat input to the generator at a rate Q_{GE} evaporates the working fluid to give a solution in the generator which is poor in working fluid. The evaporated working fluid goes to the condenser and the working fluid poor solution goes to the absorber to complete the cycle.

One of the most commonly used working fluid–absorbent pairs is water–lithium bromide. This pair has a large negative deviation from Raoult's law. Solutions which have a negative deviation from Raoult's law lower the vapour pressure by a greater amount. Conversely, for a given vapour pressure, the mole fraction of the working fluid increases with increasing

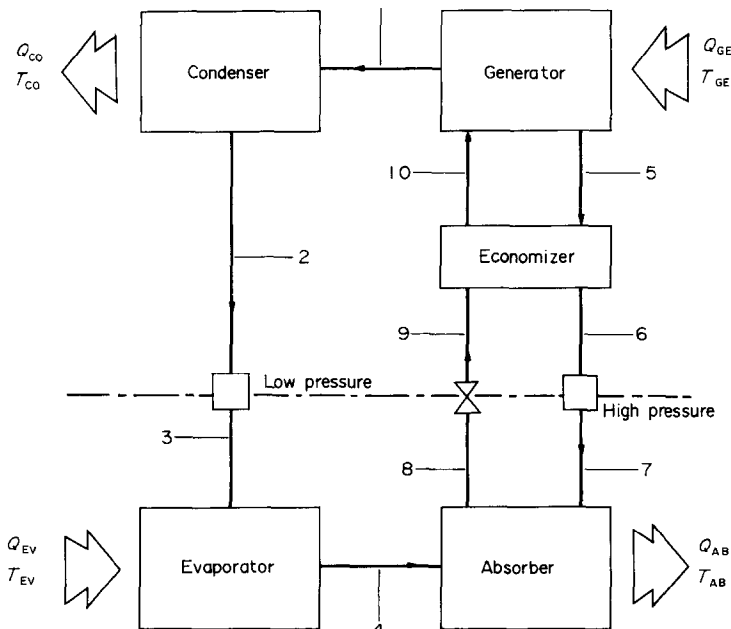


FIG. 1. Schematic diagram for a conventional absorption heat pump.

NOMENCLATURE

A	area [m ²]
C	concentration of gas in liquid [mol l ⁻¹]
C^*	equilibrium concentration of gas in liquid [mol l ⁻¹]
D	diffusion coefficient [m ² s ⁻¹]
d	diameter [m]
g	gravity acceleration constant [m s ⁻²]
K	coefficient of mass transfer [kg mol h ⁻¹ m ⁻² bar ⁻¹ or m s ⁻¹]
M	mass flow rate [kg s ⁻¹ or kg h ⁻¹]
p	partial pressure [bar]
Q	heat load [kW or kJ]
T	temperature [°C or K]
ΔT	temperature difference [K]
t	time [s]
U	overall heat transfer coefficient [W m ⁻² K ⁻¹]

z height of column [m].

Greek symbols

μ	dynamic viscosity [kg m ⁻¹ s ⁻¹]
ρ	density [kg l ⁻¹].

Subscripts

AB	absorber
CO	condenser
EV	evaporator
G	overall based on gas
GE	generator
L	overall based on liquid
l	liquid film
LM	logarithmic mean
T	inlet
V	vapour.

deviations from the law. A high negative deviation from the law has the advantage of reducing the volume flow in the secondary circuit for a given working fluid flow rate through the primary circuit.

The object of this work was to study experimentally the effect of changes in working fluid flow rate M_V on both the liquid phase mass transfer coefficient K_l and evaporator temperature T_{EV} . The aim was also to study the effect of feed rate of solution entering the absorber M_L , on the heat load Q_{EV} added to the evaporator. These parameters have a large effect on the absorption process and hence the entire efficiency of the whole system.

DESIGN OF HEAT PUMP ABSORBERS

Wetted wall absorbers have high heat transfer rates associated with the mass transfer. They also have the advantage that the interface area can be measured accurately, easily constructed and nearer to the theoretical analysis. Also it is heated where a large quantity of heat is required to be

removed. In wetted wall columns the design of the gas inlet has a considerable effect on the gas phase coefficient of performance K_g . It is several times the theoretical value due to the turbulence effect.

Vivian and Peaceman [3] related the height of the wetted wall column Z with the operating conditions by the following equation for Reynolds numbers below 2200:

$$\frac{k_l z}{D_l} = 0.433 \left(\frac{\mu_l}{\rho_l D_l} \right)^{1/2} \left(\frac{\rho_l^2 g Z^3}{\mu_l^2} \right) \left(\frac{4M_L}{\mu_L} \right)^{0.4} \quad (3)$$

where

$$K_l = \sqrt{6/\pi} \sqrt{(D_l/\rho B^2)} \quad (4)$$

and

$$B = (3\mu_l M_l / \rho_l^2 g)^{1/3}. \quad (5)$$

Astarita [4] related the height of the wetted wall column to the operating conditions including the lifetime of a liquid

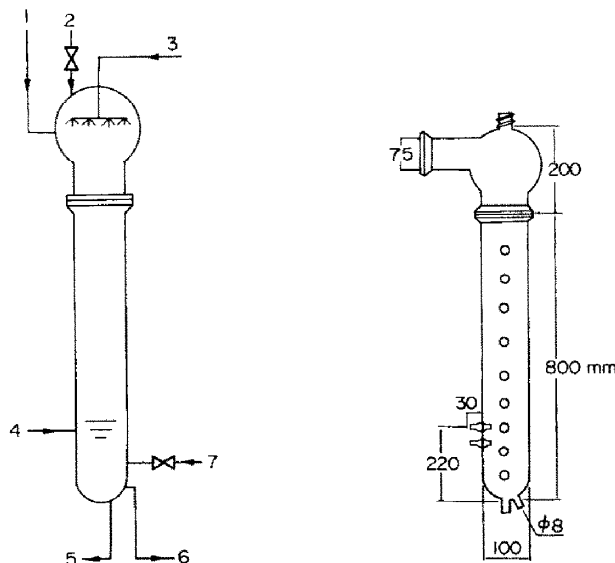


FIG. 2. The experimental absorber: 1, vapour from evaporator; 2, charging of solution; 3, solution to absorber after the external cooler; 4, solution from generator; 5, solution to generator; 6, circulation to absorber through the external cooler; 7, transfer line from evaporator to avoid crystallization.

surface element t by the following equation :

$$t = 2/3z[(\pi d/M_L)^2 3\mu_L/g\rho_L]^{1/3} \quad (6)$$

where

$$K_1 = 2\sqrt{(D/\pi t)} \quad (7)$$

and

$$K_1 = M_G/(C^* - C) \quad (8)$$

where M_G is the flow rate per unit cross-sectional area.

In the case of cooling the absorber by an inside arrangement, cooling coils can be assumed as Rashig rings and the flooding line for the specified conditions can be checked.

EXPERIMENTAL HEAT AND MASS TRANSFER STUDIES ON A GLASS ABSORPTION COOLER

The experiments were carried out in a glass absorption cooler which was constructed for the most part from standard items supplied by Quickfit Ltd, U.K.

Details of the equipment and operating techniques have already been published [5]. Figure 2 shows a sketch of the experimental absorber used.

The absorber in this unit is a spray type 1 m long and 0.1 m in diameter. The absorber head consisted of a stainless steel shower. The shower end was secured to the absorber by a vacuum screwthread cap joint placed on a screwthread glass tube welded to the top of the absorber head. The water vapour and the liquid spray fluid cocurrent rather than counter-current in order to minimize entrainment and take advantages of the small pumping action of the spray. This experiment was to study the effect of the absorbent and the vapour flow rate on the performance of the absorber, the cooling temperature T_{EV} and the cooling capacity Q_{EV} . The working fluid was water vapour and the absorbent was lithium bromide.

RESULTS AND DISCUSSIONS

Figures 3-5 are the experimental results which were obtained using the absorber shown in Fig. 2.

Figure 3 is a plot of the liquid phase mass transfer coefficient against the vapour flow rate M_V . The mass flow rates of the vapour were estimated using enthalpies H_3 and H_4 for the different measured values of evaporator load Q_{EV} ($M_V = Q_{EV}/(H_4 - H_3)$). The mass transfer coefficient K_1 was

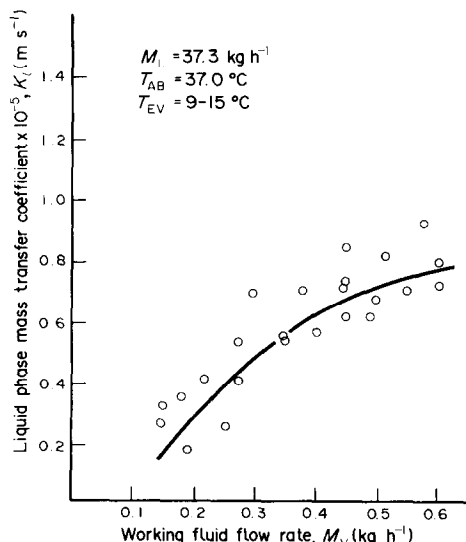


FIG. 3. Liquid phase mass transfer coefficient vs working fluid vapour flow rate.

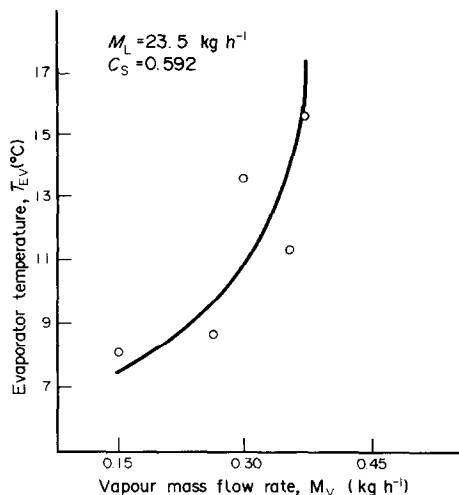


FIG. 4. Evaporator temperature vs vapour mass flow rate.

estimated from equation (8) using experimental values for concentrations and water vapour flow rate. It can be seen from Fig. 3 that the liquid phase mass transfer coefficient increases with the mass flow rate of the vapour. This is because, as the mass flow rate of vapour increases the concentration of vapour in liquid increases.

The investigation of the effect of the liquid absorbent flow rate M_L on the liquid phase mass transfer coefficient has been made using equations (6) and (7) using measured values M_L and with a typical diffusion coefficient of $2 \times 10^{-9} \text{ m}^2 \text{ s}^{-1}$ [6].

The calculated values of K_1 using the two mentioned equations have not shown a specific trend of change with M_L as it was expected to increase.

The values of the physical parameters in equation (6) were taken from published data [7, 8] corresponding to the operating conditions. Figure 4 shows the increase in evaporator temperature T_{EV} with the mass flow rate of the vapour. The rate of increase is higher at higher mass flow rates of the vapour.

Figure 5 shows the increase in cooling load Q_{EV} with an increase in liquid mass flow rate M_L entering the absorber. This is because as the mass flow of the absorbent increases, the amount of absorbed working fluid from the evaporator increases and hence the cooling capacity increases.

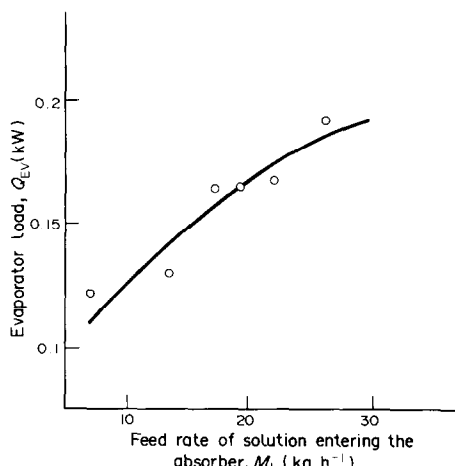


FIG. 5. Evaporator load vs feed rate of the solution entering the absorber.

CONCLUSION

Heat and mass transfer for the main equipment in absorption heat pumps have been discussed together with the design aspects for the absorbers.

The mass flow rate of the working fluid vapour has shown a significant effect on the liquid phase mass transfer coefficient and the cooling temperature in the evaporator. The cooling capacity of the absorption system has been shown to increase with increases in the mass flow rate of the aqueous lithium bromide solution used as an absorbent.

REFERENCES

1. D. B. Spalding, *Convective Mass Transfer, An Introduction*. Edward Arnold, London (1963).
2. S. Gabsi and R. Bugrel, Water absorption by a solution of lithium bromide, *Int. Commun. Heat Mass Transfer* **10**, 49 (1983).

3. J. E. Vivian and D. W. Peaceman, Liquid-side resistor in gas absorption, *J. Am. Inst. Chem. Engrs* **2**, 437 (1956).
4. G. Astarita, *Mass Transfer with Chemical Reaction*. Elsevier, London (1967).
5. M. A. R. Eisa, S. Devotta and F. A. Holland, A study of economiser performance in a water-lithium bromide cooler, *Int. J. Heat Mass Transfer* **28**, 2323 (1985).
6. I. E. Smith, Heat pump absorbers, *Proc. NATO Advanced Study Institute on Heat Pump Fundamentals*, Espinho, Spain, Sept., pp. 1-12 (1980).
7. S. A. Bogatykh and I. D. Eaovich, A study of the viscosities of aqueous solutions of LiCl, LiBr and CaCl₂ applicable to the normal drying of gases, *J. Appl. Chem. U.S.S.R.* **36**, 180 (1965).
8. S. A. Bogatykh and I. D. Eaovich, Investigation of densities of aqueous solutions of LiCl, LiBr and CaCl₂ in relation to conditions of gas drying, *J. Appl. Chem. U.S.S.R.* **38**, 932 (1965).

Int. J. Heat Mass Transfer. Vol. 34, No. 3, pp. 894-897, 1991
Printed in Great Britain

0017-9310/91 \$3.00+0.00
Pergamon Press plc

A suitable approximate solution of Neumann's problem

DIDIER LECOMTE and JEAN-CHRISTOPHE BATSALE

L.E.M.T.A., U.R.A. C.N.R.S. 875, Ecole des Mines, Parc de Saurupt, 54000 Nancy Cedex, France

(Received 15 December 1989 and in final form 9 April 1990)

1. INTRODUCTION

MOVING boundary problems have few exact analytical solutions. The most famous one was expressed by Neumann in the previous century. We will briefly report his results [1].

The problem considers a semi-infinite body of phase-change material extending from $x = 0$ to ∞ . The initial temperature T_i is assumed to be uniform and higher than the solidification temperature T_c . Dirichlet's condition is applied to the fixed boundary at a temperature T_0 ($T_0 < T_c$). Crystallization is observed and if one assumes only conductive heat transfer in both phases, the position of the boundary layer may be expressed by

$$s = 2K_N \sqrt{(a_1 t)} \quad (1)$$

The temperature profiles in the solid and the liquid phases are

$$0 < x < s(t) \quad T_1(x, t) = T_0 + \frac{(T_c - T_0)}{\operatorname{erf}(K_N)} \operatorname{erf}\left(\frac{x}{2\sqrt{(a_1 t)}}\right) \quad (2)$$

$$x > s(t) \quad T_2(x, t) = T_i - \frac{(T_i - T_c)}{\operatorname{erfc}(K_N \alpha)} \operatorname{erfc}\left(\frac{x}{2\sqrt{(a_2 t)}}\right) \quad (3)$$

where K_N is a function of three dimensionless parameters:

$$Ste = \frac{\rho_1 C_1 (T_c - T_0)}{\rho_1 L}$$

Stefan number (ratio of the sensible heat in the solid phase to the latent heat released by crystallization);

$$\phi = \frac{\rho_2 C_2 (T_i - T_c)}{\rho_1 C_1 (T_c - T_0)}$$

ratio of the sensible heat in the liquid phase to the sensible heat in the solid phase;

$$\alpha = \sqrt{(a_1/a_2)}$$

square root of the ratio of the thermal diffusivities. The solution of the transcendent equation is K_N

$$\frac{e^{-K_N^2}}{\operatorname{erf}(K_N)} - \frac{e^{-K_N^2 \alpha^2}}{\operatorname{erfc}(K_N \alpha)} \frac{\phi}{\alpha} = \frac{K_N \sqrt{\pi}}{Ste} \quad (4)$$

Equation (4) can be solved numerically but the solution can be fairly difficult to obtain when the function $\operatorname{erfc}(K_N \alpha)$ is near zero.

For various boundary conditions or various geometries, it is useful to have approximate solutions. Several methods were developed for the case where the initial overheating is zero ($\phi = 0$). In this particular case, the thermal properties of the liquid phase do not appear in the solution.

The quasi-steady approximation [2] assumes a linear profile of the temperature in the solid region and is only valid for very small Stefan numbers. For larger Stefan numbers, higher order polynomial approximations have to be used. The coefficients are determined so as to satisfy the boundary conditions. The heat equation should also be satisfied either in its integral form [3] or at a number of discrete points [3-5].

For small but non-negligible Stefan numbers, perturbation methods also yield good results [6, 7].

To find approximate solutions for the case $\phi \neq 0$, it is necessary to make assumptions on temperature profiles in both phases [8-11]. The solution is seldom simple and it is often preferable to use numerical methods [12], which allow for instance, the practical choice of the initial conditions.

In the present paper, we intend to show how a correct choice of an approximate solution may yield accurate results. In the case of Neumann's problem, the approximate solution has a very simple form and may easily be compared to the exact one.

2. STATEMENT OF THE PROBLEM

The equations for Neumann's problem are well known.

• Solid phase

$$0 < x < s(t), \quad \frac{\partial T_1}{\partial t} = a_1 \frac{\partial^2 T_1}{\partial x^2} \quad (5)$$